Phosphorylation of Tyr-398 and Tyr-402 in Occludin Prevents Its Interaction with ZO-1 and Destabilizes Its Assembly at the Tight Junctions*

Bertha C. Elias[‡], Takuya Suzuki[‡], Ankur Seth[‡], Francesco Giorgianni[§], Gautam Kale[‡], Le Shen[¶], Jerrold R. Turner[¶], Anjaparavanda Naren[‡], Dominic M. Desiderio[§], and Radhakrishna Rao[‡1]

From the [‡]Department of Physiology, [§]Charles B. Stout Neuroscience Mass Spectrometry Laboratory, University of Tennessee Health Science Center, Memphis, Tennessee 38163 and the [¶]Department of Pathology, University of Chicago, Chicago Illinois 60637

Occludin is phosphorylated on tyrosine residues during the oxidative stress-induced disruption of tight junction, and *in vitro* phosphorylation of occludin by c-Src attenuates its binding to ZO-1. In the present study mass spectrometric analyses of C-terminal domain of occludin identified Tyr-379 and Tyr-383 in chicken occludin as the phosphorylation sites, which are located in a highly conserved sequence of occludin, YETDYTT; Tyr-398 and Tyr-402 are the corresponding residues in human occludin. Deletion of YETDYTT motif abolished the c-Src-mediated phosphorylation of occludin and the regulation of ZO-1 binding. Y398A and Y402A mutations in human occludin also abolished the c-Src-mediated phosphorylation and regulation of ZO-1 binding. Y398D/Y402D mutation resulted in a dramatic reduction in ZO-1 binding even in the absence of c-Src. Similar to wild type occludin, its Y398A/Y402A mutant was localized at the plasma membrane and cell-cell contact sites in Rat-1 cells. However, Y398D/Y402D mutants of occludin failed to localize at the cell-cell contacts. Calcium-induced reassembly of Y398D/Y402D mutant occludin in Madin-Darby canine kidney cells was significantly delayed compared with that of wild type occludin or its T398A/T402A mutant. Furthermore, expression of Y398D/Y402D mutant of occludin sensitized MDCK cells for hydrogen peroxide-induced barrier disruption. This study reveals a unique motif in the occludin sequence that is involved in the regulation of ZO-1 binding by reversible phosphorylation of specific Tyr residues.

Epithelial tight junctions (TJs)[2] form a selective barrier to the diffusion of toxins, allergens, and pathogens from the external environment into the tissues in the gastrointestinal tract, lung,

liver, and kidney (1). Disruption of TJs is associated with the gastrointestinal diseases such as inflammatory bowel disease, celiac disease, infectious enterocolitis, and colon cancer (2–4) as well as in diseases of lung and kidney (5, 6). Numerous inflammatory mediators such as tumor necrosis factor α, interferon γ, and oxidative stress (7–12) are known to disrupt the epithelial TJs and the barrier function. Several studies have indicated that hydrogen peroxide disrupts the TJs in intestinal epithelium by a tyrosine kinase-dependent mechanism (11, 12).

Four types of integral proteins, occludin, claudins, junctional adhesion molecules, and tricellulin are associated with TJs. Occludin, claudins, and tricellulin are tetraspan proteins, and their extracellular domains interact with homotypic domains of the adjacent cells (1, 2, 13). The intracellular domains of these proteins interact with a variety of soluble proteins such as ZO-1, ZO-2, ZO-3, 7H6, cingulin, and symplekin (14–23); this protein complex interacts with the perijunctional actomyosin ring. The interactions among TJ proteins are essential for the assembly and the maintenance of TJs. Therefore, regulation of the interactions among TJ proteins may regulate the TJ integrity. A significant body of evidence indicates that numerous signaling molecules are associated with the TJs. Protein kinases and protein phosphatases such as protein kinase Cζ (PKCζ), PKCι/λ (24), c-Src (25), c-Yes (26, 27), mitogen-activated protein kinase (28), PP2A, and PP1 (29) interact with TJs, indicating that TJs are dynamically regulated by intracellular signal transduction involving protein phosphorylation. Additionally, other signaling molecules such as calcium (30), phosphatidylinositol 3-kinase (31), Rho (32), and Rac (33) are involved in the regulation of TJs.

Occludin, a ~65-kDa protein, has been well characterized to be assembled into the TJs. Although occludin knock-out mice showed the formation of intact TJs in different epithelia (34), numerous studies have emphasized that it plays an important role in the regulation of TJ integrity. Occludin spans the membrane four times to form two extracellular loops and one intracellular loop, and the N-terminal and C-terminal domains hang into the intracellular compartment (35–37). In epithelium with intact TJs, occludin is highly phosphorylated on Ser and Thr residues (38), whereas Tyr phosphorylation is undetectable. However, the disruption of TJs in Caco-2 cell monolayers by oxidative stress and acetaldehyde leads to Tyr phosphorylation of occludin; the tyrosine kinase inhibitors attenuate the disruption of TJs (39, 40). Furthermore, a previous *in vitro* study dem-

[1] To whom correspondence should be addressed: Dept. of Physiology, University of Tennessee, 894 Union Ave., Memphis, TN 38163. Tel.: 901-448-3235; Fax: 901-448-7126; E-mail: rkrao@physio1.utmem.edu.

[2] The abbreviations used are: TJ, tight junction; HRP, horseradish peroxidase; ZO-1, ZO-2, and ZO-3, zonula occludens 1, 2, and 3; GST, glutathione S-transferase; p-Tyr, phosphotyrosine; GFP, green fluorescence protein; TPCK, tosylphenylalanyl chloromethyl ketone; MDCK, Madin-Darby canine kidney cells; MALDI-TOF, matrix-assisted laser desorption ionization time-of-flight; WT, wild type; LC/MS/MS, liquid chromatography/tandem mass spectroscopy.

onstrated that Tyr phosphorylation of the C-terminal domain of occludin leads to the loss of its interaction with ZO-1 and ZO-3 (25).

In the present study we identified the Tyr residues in occludin that are phosphorylated by c-Src and determined their role in regulated interaction between occludin and ZO-1 and its assembly into the TJs. Results show that 1) Tyr-379 and Tyr-383 in chicken occludin and Tyr-398 and Tyr-402 in human occludin are the exclusive sites of phosphorylation by c-Src, and these Tyr residues are located in a highly conserved sequence of occludin, YET-DYTT, 2) deletion of YEDTYTT or point mutation of Tyr-398 and Tyr-402 in human occludin attenuates the phosphorylation-dependent regulation of ZO-1 binding, 3) Y398D/Y402D mutation of human occludin leads to loss of ZO-1 binding and prevents its translocation to the plasma membrane and cell-cell contact sites in Rat-1 cells, 4) Y398D/Y402D mutation of occludin delays its assembly into the intercellular junctions during the calcium-induced assembly of TJs, and 5) expression of Y398D/Y402D mutant occludin sensitizes cell monolayers for hydrogen peroxide-induced disruption of barrier function.

EXPERIMENTAL PROCEDURES

Chemicals

Cell culture reagents and supplies, G418, Lipofectamine-R, and Plus reagent were purchased from Invitrogen. FuGENE was purchased from Roche Diagnostics, and glutathione (GSH), leupeptin, aprotinin, pepstatin A, phenylmethylsulfonyl fluoride, protease inhibitor mixture, GSH-agarose, Triton X-100, and vanadate were purchased from Sigma. The QuikChange XL site-directed mutagenesis kit was from Stratagene, La Jolla, CA. Active c-Src (recombinant protein) was purchased from Upstate Biotechnology, Inc. (Lake Placid, NY). All other chemicals were of analytical grade and were purchased either from Sigma or Fisher.

Plasmids and Recombinant Proteins

cDNA for the C-terminal tail of chicken occludin (amino acids 358–504) was a kind gift from Dr. James Anderson (University of North Carolina, Chapel Hill, NC); this was used to amplify and insert into pGEX2T vector. The C-terminal tail of human occludin 378–522 was amplified from a full-length human occludin in pEGFP and then shuttled into pGEX2T vector. Site directed mutations were induced in both chicken and human occludin (C-terminal domain as well as full-length occludin). The sequences of the primers used for this are provided in Table 1. The mutations were confirmed by sequencing. pGEX2T constructs containing wild type occludin C-terminal domain (GST-cOcl-C and GST-hOcl-C) were transformed into BL21DE3 cells, and recombinant proteins were purified. The full-length human occludin (wild type and mutants) in pEGFP vector was used for transfection into Rat-1 and MDCK cells.

Mass Spectrometric Analysis

Trypsin Digestion—GST-cOcl-C$_{WT}$, tyrosine-phosphorylated by c-Src, was suspended in 10% acetonitrile in 10 mM ammonium bicarbonate, pH 8.5, and incubated at 37 °C overnight with TPCK-treated trypsin (enzyme to substrate molar ratio of 1:10). The

TABLE 1

Sequences of primers used to generate various mutations

Sequences in bold substitute tyrosine residues in the wild type occludin.

Predicted mutant	Forward primer sequence 5′–3′
Chicken occludin	
Δ378–385	CCCGAGTTGGATGAGTCCGCCGTGGAGTCCAGTGAT
Y379A	TGGATGAGTCCCAG**GCT**GAGACCGACTAC
Y379F	TGGATGAGTCCCAG**TTT**GAGACCGACTAC
Y379D	TGGATGAGTCCCAG**GAT**GAGACCGACTAC
Y383A	GTATGAGACCGAC**GCC**ACCACGGCCG
Y383F	GTATGAGACCGAC**TTC**ACCACGGCCG
Y383D	GTATGAGACCGAC**GAC**ACCACGGCCG
Y379/383A	GGATGAGTCCCAG**GCT**GAGACCGAC**GCC**ACCACGGCCGTGG
Y379/383F	GGATGAGTCCCAG**TTT**GAGACCGAC**TTC**ACCACGGCCGTGG
Y379/383D	GGATGAGTCCCAG**GAT**GAGACCGAC**GAC**ACCACGGCCGTGG
Human occludin	
Y398A	GAGAACAGAGCAAGATCAC**GCT**GAGACAGACTACACAACTGG
Y402A	GCAAGATCACTATGAGACAGAC**GCC**ACAACTGGCGGCGAGTCCTG
Y398/402A	CAGAGCAAGATCAC**GCT**GAGACAGAC**GCC**ACAACTGGCGGCGAG
Y398F	GAGAACAGAGCAAGATCAC**TTT**GAGACAGACTACACAACTGG
Y402F	GCAAGATCACTATGAGACAGAC**TTC**ACAACTGGCGGCGAGTCCTG
Y398/402F	CAGAGCAAGATCAC**TTT**GAGACAGAC**TTC**ACAACTGGCGGCGAG
Y398D	GAGAACAGAGCAAGATCAC**GAT**GAGACAGACTACACAACTGG
Y402D	GCAAGATCACTATGAGACAGAC**GAC**ACAACTGGCGGCGAGTCCTG
Y398/402D	CAGAGCAAGATCAC**GAT**GAGACAGAC**GAC**ACAACTGGCGGCGAG

digest was passed through 0.45-μm filters. Clear supernatant was lyophilized to dryness. Air-dried samples were equilibrated in an aqueous solution containing 0.1% trifluoroacetic acid and desalted by passing through C-18 ZipTip (Millipore, Bedford, MA) using the manufacturer's protocol. Peptides extracted from the ZipTip were subjected to phosphopeptide extraction.

Extraction of Phosphopeptides—The phosphopeptides from trypsin digestion of Tyr-phosphorylated GST-cOcl-C were isolated using a phosphopeptide isolation kit (Pierce). Phosphopeptides were bound to immobilized gallium matrix at acidic pH ($<$3.5) and eluted in 50 mM ammonium bicarbonate at pH 10. Phosphopeptide extracts were then subjected to MALDI and LC/MS/MS analysis.

MALDI-TOF—Phosphopeptide extracts were dried under vacuum and reconstituted in 2 μl of matrix (α-cyano-4-hydroxycinnamic acid) and spotted for crystallization. Crystals were analyzed for mass by MALDI-TOF using Voyager Biospectrometry work station DE (delayed extraction technology) (Perspective Biosystems Inc., Framingham, MA) and Data Explorer (Perspective Biosystems). A Prescriptive Biosystems MALDI time-of-flight instrument incorporating a nitrogen laser (Laser Science, Newton, MA) was used to obtain MALDI mass spectra. Samples solubilized in 85% acetic acid and mixed (1:3 v/v) with α-cyano-4-hydroxycinnamic acid matrix were spotted in 1-μl aliquots and air-dried. Typically, 100–250 laser shots were used to obtain one mass spectrum. Mass scale was calibrated with peptide internal standards.

LC/MS/MS Analysis—Sequence analysis of tryptic peptides was performed by injecting 3 μl of the ZipTip-purified sample onto a capillary C-18 LC column on-line with a Finnigan LCQ[DECA] (Thermoquest, San Jose, CA) ion-trap mass analyzer that is equipped with a nanoelectrospray ionization source. The capillary C-18 column was prepared in-house using New Objective Pico Frit (360-μm outer diameter, 75-μm inner diameter, 15-μm tip, 10.4-cm length) and Magic C18AQ packing material (5-μm beads, 200 A° pores). The peptides were fractionated using 0.1% formic acid in water as solvent A and 90% acetonitrile as solvent B. The acquired spectra were visualized using Qual-browser in the X-Calibur software suite. Raw

data thus obtained was analyzed against a protein data base generated from Swissprot using the Sequest software suite (Sequest Technologies Inc., Lisle, IL).

Antibodies—Mouse monoclonal anti-ZO-1, rabbit polyclonal anti-ZO-1, and rabbit polyclonal anti-ZO-3 were purchased from Zymed Laboratories Inc., and AlexaFluor 488-conjugated anti-mouse IgG antibody was from Molecular Probes (Eugene, OR). Anti-phosphotyrosine antibody conjugated with horseradish peroxidase (HRP) was from BD Transduction Laboratories. HRP-conjugated mouse monoclonal anti-GST antibody was from Upstate Biotechnology. Cy3-conjugated anti-rabbit IgG, HRP-conjugated anti-mouse IgG, and HRP-conjugated anti-rabbit IgG antibodies were purchased from Sigma.

Cell Culture and Transfection

Caco-2, Rat-1, and MDCK cells were cultured in Dulbecco's modified Eagle's medium from Invitrogen and supplemented with 10% fetal bovine serum, 1 mM sodium pyruvate, and 2 mM glutamine as per the ATCC guidelines. MDCK cells were seeded on 6-well plates a day before transfection to achieve 50–60% confluency. The cells were transfected using 1 ml of antibiotic-free Dulbecco's modified Eagle's medium containing 10% fetal bovine serum, 1 μg of DNA plasmid (empty vector pEGFP or vector carrying hOcl$_{WT}$ or its mutants), 1 μl of Plus reagent, and 3 μl of Lipofectamine-R for each well. After 20 h, the cell monolayers were trypsinized and seeded onto 100-mm plates. The cells were subjected to G418 selection (0.7 mg/ml) for 2 weeks. Resistant cells were sorted to obtain only GFP-expressing cells by fluorescence-activated cell sorter. Cells were maintained in the medium that was supplemented with 0.3 mg/ml G418. Rat-1 cells were transfected using FuGENE reagent as per the manufacturer's protocol, and the GFP-positive cells were sorted by fluorescence-activated cell sorter. Stably transfected cells were selected using G418 as described above.

Immunofluorescence Microscopy

Cell monolayers (12-mm transwells) were washed with phosphate-buffered saline and fixed in acetone-methanol (1:1) at 0 °C for 5 min. Cell monolayers were blocked in 3% nonfat milk in TBST (20 mM Tris, pH 8.0, containing 150 mM NaCl and 0.5% Tween 20) and incubated for 1 h with primary antibodies (rabbit polyclonal anti-ZO-1 and mouse monoclonal anti-GFP) followed by incubation for 1 h with secondary antibodies (Cy3-conjugated anti-rabbit IgG and AlexaFluor 488-conjugated anti-mouse IgG). The fluorescence was visualized using a Zeiss LSM 5 laser scanning confocal microscope, and images from Z-series sections (1 μm) were collected by using Zeiss LSM 5 Pascal Confocal Microscopy Software (Release 3.2). Images were stacked using the software, Image J (NIH), and processed by Adobe Photoshop (Adobe Systems Inc., San Jose, CA).

Occludin Phosphorylation in Vitro

Recombinant GST-cOcl-C$_{WT}$ or GST-hOcl-C$_{WT}$ (5 μg) was incubated with 500 ng of active c-Src in 250 μl of kinase buffer (50 mM Hepes, pH 7.4, 1 mM EDTA, 0.2% β-mercaptoethanol, 3 mM MgCl$_2$) containing 100 μM ATP at 30 °C for 3 h on a shaking incubator. Control reactions were done in the absence of ATP.

GST Pulldown Assay

To determine the interaction of occludin with ZO-1 and ZO-3, GST-hOcl-C GST-cOcl-C (2.5–10 μg) was incubated with Caco-2 whole cell extract made in phosphate-buffered saline containing 0.2% Triton X-100, 1 mM sodium vanadate, and 10 mM sodium fluoride for 16 h at 4 °C on an inverter. GST-occludin-C (GST-conjugated C-terminal tail of occludin) was pulled down with 20 μl of 50% GSH-agarose slurry at 4 °C for 1 h. The amounts of ZO-1 and ZO-3 bound to GSH-agarose were determined by immunoblot analysis. Nonspecific binding was determined by carrying out the binding with GST.

Immunoblot and Densitometric Analysis

Proteins were separated by 7% SDS-polyacrylamide gel electrophoresis and transferred to polyvinylidene difluoride membranes. Membranes were blotted for ZO-1, ZO-3, and p-Tyr by using specific antibodies in combination with HRP-conjugated anti-mouse IgG or HRP-conjugated anti-rabbit IgG antibodies. HRP-conjugated anti-GST antibody was used for immunoblot analysis of GST or GST-occludin. The blot was developed using ECL chemiluminescence method (Amersham Biosciences). Quantitation was performed by densitometric analysis of specific bands on immunoblots by using the software, Image J.

Hydrogen Peroxide Treatment and Paracellular Permeability

MDCK cell monolayers that stably express GFP-hOcl$_{WT}$, GFP-hOcl$_{Y398A/Y402A}$, or GFP-hOcl$_{Y398D/Y402D}$ were exposed to varying concentrations (20–2500 μM) of hydrogen peroxide for 2 h, and paracellular permeability was evaluated by measuring the unidirectional flux of inulin as described before (11).

TJ Assembly by Calcium Switch

MDCK cell monolayers that stably express GFP-hOcl$_{WT}$, GFP-hOcl$_{Y398A/Y402A}$, or GFP-hOcl$_{Y398D/Y402D}$ were incubated overnight with low calcium medium followed by calcium replacement as described before (29). TJ assembly was evaluated by measuring transepithelial electrical resistance, inulin permeability, and confocal microscopy.

Immunoprecipitation

GFP was immunoprecipitated from cells under native or denatured conditions as described before (29). Anti-GFP immunocomplexes at native conditions were immunoblotted for ZO-1, whereas complexes under denatured conditions were immunoblotted for p-Tyr.

Statistics

Comparison between two groups was made by Student's *t* tests for grouped data. Significance in all tests was set at 95% or greater confidence level.

RESULTS

Tyr-379 and Tyr-383 in Chicken Occludin Are the Sites of Phosphorylation by c-Src—A previous study showed that Tyr phosphorylation of occludin C-terminal domain by c-Src resulted in the loss of its interaction with ZO-1 (25). In the present study we identified the phosphorylation sites in occlu-

din C-terminal domain by mass spectrometric analysis. GST-fused C-terminal region (150 amino acids) of chicken occludin (GST-cOcl) was prepared and phosphorylated by incubation with c-Src and ATP. Tyr-phosphorylated GST-cOcl-C was digested with trypsin. Generation of five different tryptic peptides containing Tyr residues was predicted (Fig. 1A); the mass of these peptides was expected to increase by 80 Da with phosphorylation of each Tyr residue. MALDI mass spectrometric analysis of the phosphopeptide extracts from the tryptic digest detected several phosphopeptides with masses slightly deviated from the predicted mass analysis (Fig. 1*B*). Fig. 1*C* shows the ion fragmentation spectrum from LC/MS/MS analysis of the phosphopeptide with a mass of 2918 Da. The sequences of peptides as determined by LC/MS/MS analyses of the phosphopeptide extract are summarized in Fig. 1*D*. Three different Tyr-phosphorylated peptides were identified. All three peptides were identified as the derivatives of tryptic peptide, P1 with single or double phosphorylation of Tyr residues. These results determine that two Tyr residues in occludin C-terminal region corresponding to the sequence of P1 were singly or doubly phosphorylated. These two Tyr residues correspond to Tyr-379 and Tyr-383 in chicken occludin.

Sequence alignment of occludin from different species (Fig. 2*A*) demonstrated that Tyr-379 and Tyr-383 are located in a highly conserved sequence of occludin (YETDYTT) and that Tyr-398 and Tyr-402 are the corresponding Tyr residues in human occludin. Therefore, we induced mutations in chicken and human occludin C-terminal region (cOcl-C and hOcl-C). The YETDYTT was deleted or the tyrosine residues in this region were subjected to point mutation in cOcl-C and hOcl-C (Fig. 2*B*) and inserted into pGEX2T vector to generate GST-fused mutant proteins. Tyr-398 and Tyr-402 in full-length human occludin in pEGFP vector were mutated to phenylalanine or aspartic acid and expressed in Rat-1 or MDCK cells as GFP fusion proteins.

A

	Position	Sequence	Mass (Da)
P1	371-393	NPELDESQ**Y**ETD**Y**TTAVESSDER	2678.6
P2	446-467	LDSITEDSPQ**Y**QDAVAEE**Y**NQLK	2585.7
P3	394-411	DQEQWASL**Y**PPITSDGAR	2034.1
P4	472-478	SPD**Y**QSK	823.8
P5	495-501	MVSA**Y**DK	812.9

B

C

D
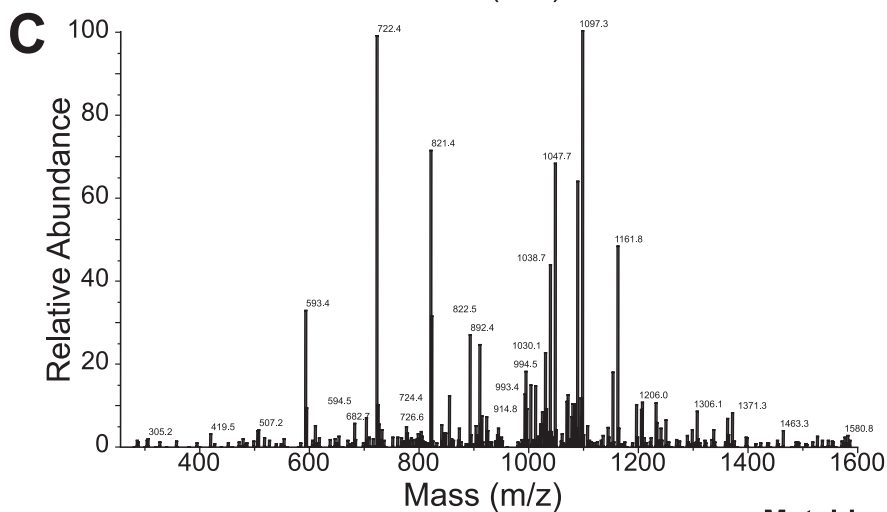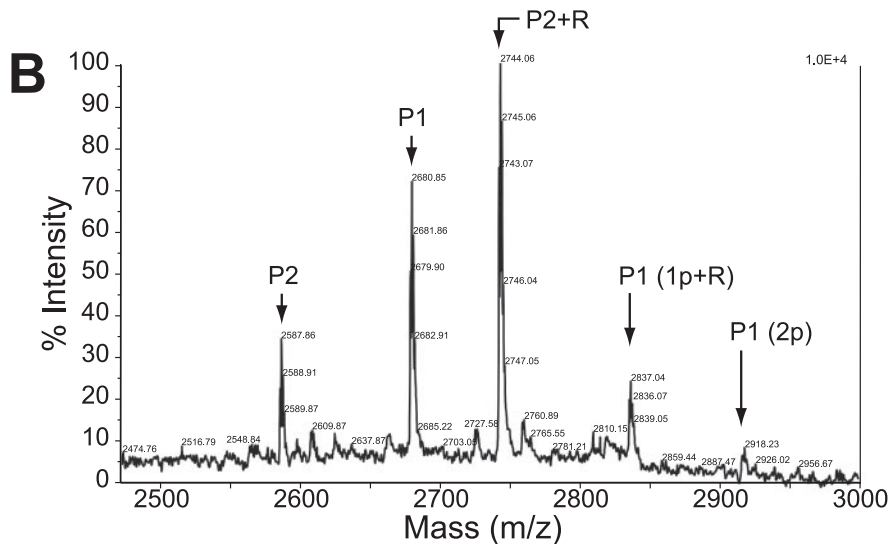
	Mass	Sequence	Matching peptide
	2679.1	NPELDESQ**Y**ETD**Y**TTAVESSDER	P1
	2742.3	RLDSITEDSPQ**Y**QDVAEE**Y**NQLK	P2+R
	2915.2	RNPELDESQ**Y**ETD**Y***TTAVESSDER	P1+R(1PO4)
	2586.5	LDSITEDSPQ**Y**QDVAEE**Y**NQLK	P2
	2835.2	RNPELDESQ**Y**ETD**Y**TTAVESSDER	P1+R
	2034.5	DQEQWASL**Y**PPITSDGAR	P3
	2915.7	RNPELDESQ**Y***ETD**Y**TTAVESSDER	P1+R(1PO4)
	2839.3	NPELDESQ**Y***ETD**Y***TTAVESSDER	P1(2PO$)
	824.4	SPD**Y**QSK	

A

Y402 (human)
Y398 (human)

```
M.musculus     VAQEIPLTLSVDDFRQPRYSSNGNLETPSKRAPTKGKAGKGKRTDPDHYETDYTTGGESC 408
R.norvegicus   VAQEIPLTLSVDDFRQPRYSSNDNLETPSKRTPTKGKAGKGKRTDPDHYETDYTTGGESC 410
H.sapiens      VVQELPLTSPVDDFRQPRYSSGGNFETPSKRAPAKGRAGRSKRTEQDHYETDYTTGGESC 409
C.familiaris   VVQELPATSPADDFRQPRYSSGHLEPSKRAPSKGRTGRPKRLEQDHYETDYTTGGESC 408
G.gallus       RALSASPVHGEEEEEKGKDQPS---RPPARRG---RRRRRNPELDESQYETDYTTAVESS 390

M.musculus     EELEED-WVREYPPITSDQQRQLYKRNFDAGLQEYKSLQAELDDVNKELSRLDKELDDYR 467
R.norvegicus   DELEED-WLREYPPITSDQQRQLYKRNFDAGLQEYKSLLAELDEVNKELSRLDRELDDYR 469
H.sapiens      DELEED-WIREYPPITSDQQRQLYKRNFDTGLQEYKSLQSELDEINKELSRLDKELDDYR 468
C.familiaris   DELEED-WIREYPPITSDQQRQLYKRNFDTGLQEYKSLQAELDEINKELSRLDKELDDYR 467
G.gallus       DERDQEQWASLYPPITSDGARQRYKQEFDTDLKRYKQLCAEMDSINDRLNQLSRRLDSIT 450

M.musculus     EESEEYMAAADEYNRLKQVKGSADYKSKRNYCKQLKSKLSHIKRMVGDYDRRKP 521
R.norvegicus   EESEEYMAAADEYNRLKQVKGSADYKSKNYCKQLKSKLSHIKRMVGDYDRRKT 523
H.sapiens      EESEEYMAAADEYNRLKQVKGSADYKSKNHCKQLKSKLSHIKKMVGDYDRQKT 522
C.familiaris   EESEEYMAAADEYNRLKQVKGSPDYKNRNYCKQLKSKLSHIKKMVGDYDRQKT 521
G.gallus       EDSPQYQDVAEEYNQLKDLKRSPDYQSKKQESKVLRNKLFHIKRMVSAYDKVRG 504
```

B Mutations in C'terminal tail of occludin

Chicken	Human
Δ378–385	Y398D,Y402D,Y398/402D
Y379D,Y383D,Y379/383D	Y398F,Y402F,Y398/402F
Y379F,Y383F,Y379/383F	Y398A,Y402A,Y398/402A

FIGURE 2. **Mutation of occludin.** *A,* the alignment of amino acid sequence of occludin from different mammalian species indicate that the Tyr residues phosphorylated by c-Src correspond to Tyr-379 and Tyr-383 in chicken occludin and Tyr-398 and Tyr-402 in human occludin. *B,* list of the mutations induced in the C-terminal region of chicken and human occludin.

Deletion of YEDYTT in Chicken Occludin C-terminal Region Prevents Phosphorylation and Attenuates Regulation of ZO-1 Binding—The ability of GST-cOcl-C or GST-cOcl-C$_{(\Delta 378-385)}$ to bind ZO-1 was evaluated by GST pulldown assay. Both GST-cOcl-C and GST-cOcl$_{(\Delta 378-385)}$ showed dose-dependent binding to ZO-1 and ZO-3 (Fig. 3A). However, ZO-1 binding to GST-cOcl$_{(\Delta 378-385)}$ was low at higher doses compared with the ZO-1 binding to GST-cOcl-C under similar conditions (Fig. 3B). Incubation with c-Src in the presence of ATP induced Tyr phosphorylation of GST-cOcl-C, whereas no phosphorylation was detected in GST-cOcl$_{(\Delta 378-385)}$ (Fig. 3C). Incubation of GST-cOcl-C with c-Src in the presence of ATP significantly reduced ZO-1 binding (Fig. 3, C and D), whereas ZO-1 binding was similar for GST-cOcl$_{(\Delta 378-385)}$ that was incubated with c-Src in the presence or absence of ATP.

Y379F and Y383F Mutation of Chicken Occludin Attenuates Its Phosphorylation and Regulation of ZO-1 Binding—GST pulldown assay for ZO-1 binding showed that GST-cOcl-C$_{WT}$, GST-cOcl-C$_{Y379F}$, GST-cOcl-C$_{Y383F}$, and GST-cOcl-C$_{Y379F/Y383F}$ bind ZO-1 and ZO-3 in a dose-dependent manner (Fig. 4A). Incubation with c-Src in the presence of ATP showed a partial phosphorylation of single mutants, GST-cOcl-C$_{Y379F}$ and GST-cOcl-C$_{Y383F}$, whereas phosphorylation was undetectable in the double mutant, GST-cOcl-C$_{Y379F/Y383F}$ (Fig. 4B). ZO-1 binding was not significantly different among unphosphorylated occludin (Fig. 4, B and

C), except that ZO-1 binding of GST-cOcl-C$_{Y379F}$ was slightly greater than that of GST-cOcl-C$_{WT}$. Incubation in the presence of ATP and c-Src resulted in a reduced ZO-1 binding by GST-cOcl-C$_{WT}$ and GST-cOcl-C$_{Y379F}$ (Fig. 4, B and C). However, incubation with c-Src in the presence of ATP did not alter the ZO-1 binding by GST-cOcl-C$_{Y383F}$ and GST-cOcl-C$_{Y379F/Y383F}$ (Fig. 4, B and C).

Y379D and Y383D Mutation in Chicken Occludin Attenuates Its Binding to ZO-1—GST pulldown assay showed a dose-dependent binding of GST-cOcl-C$_{WT}$, GST-cOcl-C$_{Y379D}$, GST-cOcl-C$_{Y383D}$, and GST-cOcl-C$_{Y379/383D}$ to ZO-1 and ZO-3 (Fig. 5A). However, the ZO-1 binding to GST-cOcl-C$_{Y379D}$, GST-cOcl-C$_{Y383D}$, and GST-cOcl-C$_{Y379/383D}$ was significantly low as compared with ZO-1 binding to GST-cOcl-C$_{WT}$ (Fig. 5A). ZO-3 binding to GST-cOcl-C$_{Y383D}$ and GST-cOcl-C$_{Y379/383D}$ were significantly low compared with ZO-3 binding to GST-cOcl-C$_{WT}$, whereas ZO-3 binding to GST-cOcl-C$_{Y379D}$ was significantly greater. c-Src-induced Tyr-phosphorylation of GST-cOcl-C$_{Y379D}$ and GST-cOcl-C$_{Y383D}$ was low compared with Tyr phosphorylation of GST-cOcl$_{WT}$, and the Tyr-phosphorylation was absent in GST-cOcl-C$_{Y379/383D}$ double mutant (Fig. 5B). Incubation with c-Src in the presence of ATP resulted in reduced ZO-1 binding to GST-cOcl-C$_{WT}$ and GST-cOcl-C$_{Y379D}$ (Fig. 5, B and C). However, incubation of GST-cOcl-C$_{Y383D}$ and GST-cOcl-C$_{Y379/383D}$ with c-Src in the presence of ATP did not alter ZO-1 binding (Fig. 5, B and C).

Mutation of Tyr-398 and Tyr-402 in Human Occludin Prevents Phosphorylation and Alters ZO-1 Binding—The sequence analysis indicated that Tyr-398 and Tyr-402 are the residues in human occludin that correspond to Tyr-379 and Tyr-383 in chicken occludin. Therefore, we mutated Tyr-398 and Tyr-402 in hOcl-C. Similar to GST-cOcl-C$_{WT}$, incubation with c-Src in the presence of ATP induced Tyr phosphorylation of GST-hOcl-C$_{WT}$, whereas phosphorylation was undetectable in GST-hOcl-C$_{Y398F/Y402F}$ and GST-hOcl-C$_{Y398D/Y402D}$ mutants (Fig. 6A). GST pulldown assay showed that GST-hOcl-C$_{WT}$ binds to ZO-1, and this binding was reduced by incubation with c-Src in the presence of ATP. GST-hOcl-C$_{Y398D/Y402D}$ showed only a trace amount

FIGURE 1. **Identification of phosphorylation sites in occludin.** GST-cOcl-C$_{WT}$ was phosphorylated by incubation with c-Src in the presence of ATP and subjected to digestion by trypsin. *A,* predicted peptide fragments (*P1–P5*) that contained one or two Tyr residues generated by trypsin digestion of GST-cOcl-C$_{WT}$. The position of peptides in the sequence of occludin and their predicted mass are listed. *B,* phosphopeptides extracted from trypsin digests were subjected to mass analyses by MALDI mass spectrometry. *P1(1p+R)* represents P1 tryptic peptide with one phospho-Tyr and one additional Arg residue as a result of misdigestion by trypsin, and *P1(2p)* represents the P1 peptide with two phospho-Tyr residues. *C,* the ion fragmentation spectrum for P1(2p) as obtained by LC/MS/MS analyses. *D,* the summary of peptides sequenced by LC/MS/MS analysis. Peptides corresponding to these are listed in *panel A,* and their phosphorylation states are provided. *Asterisks* represent the phosphorylated Tyr residues.

A

IB: ZO-1

IB: ZO-3

IB: GST

| 1 | 2.5 | 5 | 10 | 1 | 2.5 | 5 | 10 | 5 | μg |

WT (p44)   Δ 378-385 (p42)   GST (p22)

B

□ WT
■ Δ378-385

Relative Density

ZO-1   ZO-3

C

| + | + | + | + | c-Src |
| − | + | − | + | ATP |

IB: ZO-1

IB: pY

IB: GST

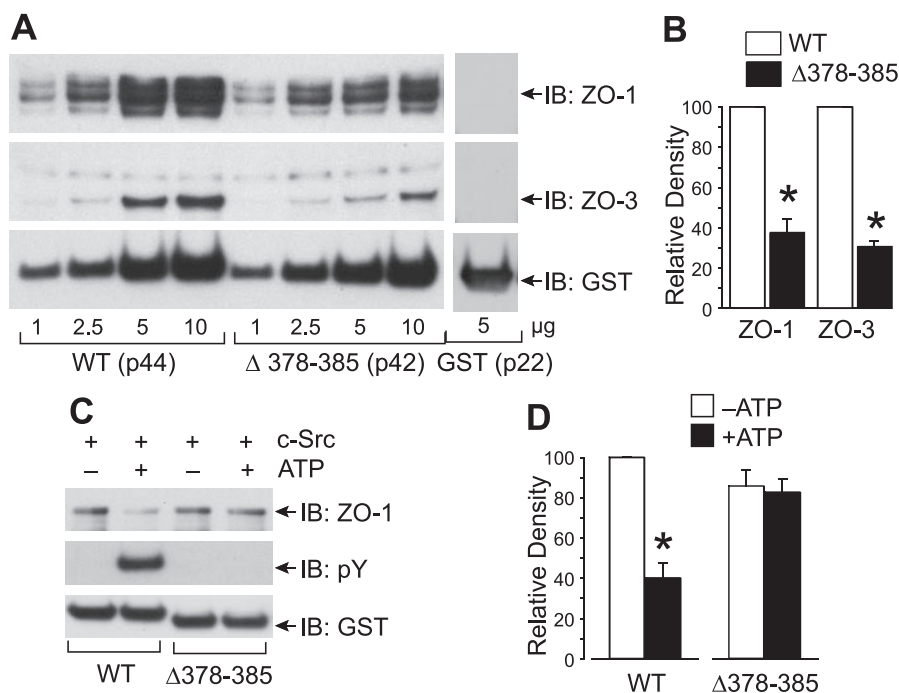WT   Δ378-385

D

□ −ATP
■ +ATP

Relative Density

WT   Δ378-385

FIGURE 3. Deletion mutation of occludin prevents phosphorylation and attenuates regulation of ZO-1 binding. *A*, varying amounts of GST-cOcl-C$_{WT}$ or GST-cOcl-C$_{(\Delta378-385)}$ was analyzed for ZO-1 binding by GST pulldown assay using Caco-2 cell extract. GST pulldown was immunoblotted (*IB*) for ZO-1, ZO-3, and GST. Binding to GST (5 μg) was performed as a control. The labels p44, p42, and p22 correspond to the molecular weight of GST-cOcl-C$_{WT}$, GST-cOcl-C$_{(\Delta378-385)}$, and GST, respectively. *B*, densitometric analysis of ZO-1 and ZO-3 binding to 5 μg of wild type (*WT*) or mutant (Δ*378–385*) occludin. Values are the mean ± S.E. (*n* = 3). *Asterisks* indicate the values that are significantly (*p* < 0.05) different from corresponding value for WT group. *C*, GST-cOcl-C and GST-cOcl-C$_{(\Delta378-385)}$, 2.5 μg, were incubated with c-Src in the absence or presence of ATP and analyzed for ZO-1 binding by GST pulldown assay. GST pulldown assays were immunoblotted for ZO-1, p-Tyr, and GST. *D*, densitometric analysis of ZO-1 bands from three different experiments described in *panel B*. In each experiment, ZO-1 band density for GST-cOcl-C$_{WT}$ incubated without ATP was designated to 100, and corresponding bands in other groups were normalized as a percent of that number. Values are the mean ± S.E. (*n* = 3). The *asterisk* indicates the value that is significantly (*p* < 0.05) different from corresponding value for −ATP group.

Tyr-398 and Tyr-402 on the distribution of occludin at the plasma membrane and the intercellular junctions, we transfected Rat-1 cells (occludin null) with GFP-hOcl, GFP-hOcl$_{Y398A/Y402A}$, and GFP-hOcl$_{Y398D/Y402D}$ and visualized the cells by confocal microscopy. GFP-hOcl$_{WT}$ and GFP-hOcl$_{Y398A/Y402A}$ were localized to both the plasma membrane and the intracellular compartment (Fig. 7). A greater level of occludin was found at the cell-cell contact sites, which was associated with the redistribution of ZO-1 at the cell-cell contact and the plasma membrane. In contrast, GFP-hOcl$_{Y398D/Y402D}$ was localized exclusively at the intracellular compartment with no trace of distribution at the plasma membrane or cell-cell contact sites (Fig. 7).

Y398D/Y402D Mutation of Occludin Delays Its Assembly at the TJs and Sensitizes MDCK Cells for TJ Disruption by Hydrogen Peroxide—Unlike Rat-1 cells, in MDCK cell monolayers, GFP-hOcl$_{Y398D/Y402D}$ appeared at the intercellular junctions. However, during the calcium switch-induced assembly of TJs, GFP-hOcl$_{Y398D/Y402D}$ localized predominantly at the intracellu-

of ZO-1 binding. ZO-1 binding to GST-hOcl-C$_{Y398F/Y402F}$ was lower than GST-hOcl-C$_{WT}$; however, the ZO-1 binding was not further reduced by incubation with c-Src in the presence of ATP (Fig. 6, *A* and *C*). Unlike reduced binding to GST-hOcl-C$_{Y398F/Y402F}$, the ZO-1 binding to GST-hOcl-C$_{Y398A/Y402A}$ was similar to that of GST-hOcl-C$_{WT}$ (Fig. 6*B*). Once again, GST-hOcl-C$_{Y398A/Y402A}$ showed no Tyr phosphorylation or regulation of ZO-1 binding when incubated with c-Src in the presence of ATP (Fig. 6*B*). Densitometric analysis (Fig. 6*C*) confirmed that ZO-1 binding to GST-hOcl-C$_{Y398A/Y402A}$ and GST-hOcl-C$_{Y398D/Y402D}$ is significantly lower than that of GST-hOcl-C$_{WT}$, whereas the binding to GST-hOcl-C$_{Y398A/Y402A}$ was similar to that of GST-hOcl-C$_{WT}$. Furthermore, incubation with c-Src in the presence of ATP significantly reduced ZO-1 binding to GST-hOcl-C$_{WT}$ but not to GST-hOcl-C$_{Y398F/Y402F}$, GST-hOcl-C$_{Y398A/Y402A}$, or GST-hOcl-C$_{Y398D/Y402D}$ when compared with corresponding ZO-1 binding in the absence of ATP.

Y398D and Y402D Mutation in Human Occludin Prevents Its Localization at Plasma Membrane and Cell-Cell Contact Sites in Rat-1 Cells—The regulation of ZO-1 binding by Tyr-398 and Tyr-402 raised the question of whether phosphorylation of Tyr-398 and/or Tyr-402 of occludin affects its localization at the TJs. To determine the effect of mutation of

lar compartment, whereas GFP-hOcl$_{WT}$ and GFP-hOcl$_{Y398A/Y402A}$ appeared at the intercellular junctions 1 h after calcium replacement (Fig. 8*A*). The inulin permeability in cell monolayers that express GFP-hOcl$_{Y398D/Y402D}$ was significantly greater than those in cell monolayers expressing GFP-hOcl$_{WT}$ or GFP-hOcl$_{Y398A/Y402A}$ (Fig. 8*B*). As reported before (11), hydrogen peroxide induced a dose-dependent increase in inulin permeability in MDCK cell monolayers that stably express GFP-hOcl$_{WT}$ (Fig. 9*A*). A hydrogen peroxide-induced increase in inulin permeability was significantly lower in cell monolayers that express GFP-hOcl$_{Y398A/Y402A}$, whereas it was significantly higher in cells expressing GFP-hOcl$_{Y398D/Y402D}$. Incubation of cell monolayers that express GFP-hOcl$_{WT}$, GFP-hOcl$_{Y398A/Y402A}$, and GFP-hOcl$_{Y398D/Y402D}$ with 500 μM hydrogen peroxide for 1 h increased inulin permeability (% flux/h/cm^2) from 0.025 ± 0.005 to 0.035 ± 0.01, 0.02 ± 0.01 to 0.025 ± 0.006, and 0.07 ± 0.007 to 0.25 ± 0.03, respectively. These observations were confirmed by analyzing the junctional distribution of GFP and ZO-1 after hydrogen peroxide treatment. Hydrogen peroxide induced a slight redistribution of GFP in cells expressing GFP-hOcl$_{WT}$, whereas the hydrogen peroxide-induced redistribution of GFP from the junctions was much more dramatic in cells that express GFP-hOcl$_{Y398D/Y402D}$
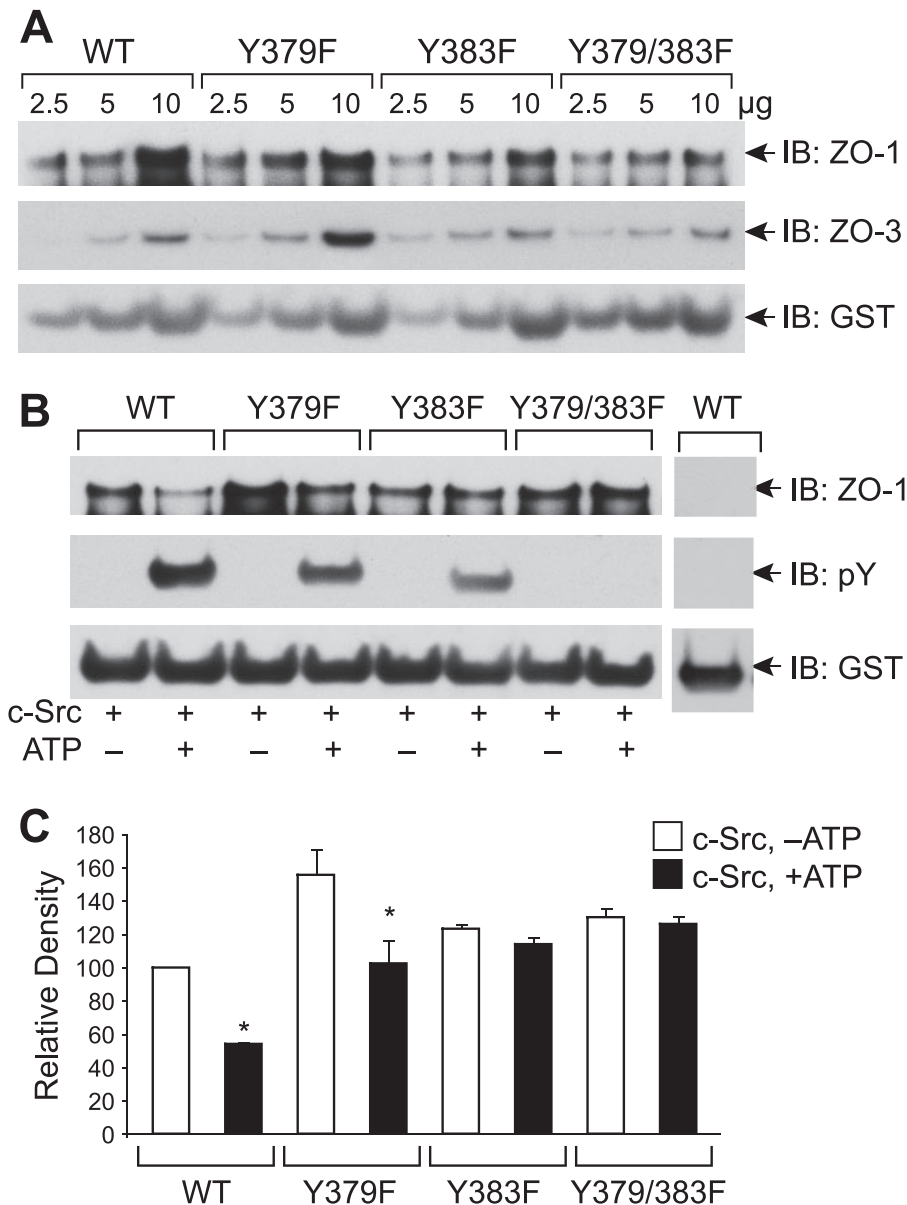
A, WT, Y379F, Y383F, Y379/383F

B, WT, Y379F, Y383F, Y379/383F, WT

C

FIGURE 4. **Y379F and Y383F mutations in chicken occludin attenuate c-Src-mediated Tyr phosphorylation and regulation of ZO-1 binding.** *A*, GST-cOcl-C$_{WT}$, GST-cOcl-C$_{Y379F}$, GST-cOcl-C$_{Y383F}$, and GST-cOcl-C$_{Y379/383F}$ were analyzed for ZO-1 binding by GST pulldown assay. GST pulldown assays were immunoblotted (*IB*) for ZO-1, ZO-3, and GST. *B*, GST-cOcl-C, GST-cOcl-C$_{Y379F}$, GST-cOcl-C$_{Y383F}$, and GST-cOcl-C$_{Y379/383F}$ were incubated with c-Src in the absence or presence of ATP. Five μg of phosphorylated and non-phosphorylated occludins were analyzed for ZO-1 binding by GST pulldown assay. GST pulldown assays were immunoblotted for ZO-1, p-Tyr, and GST. Control binding was performed by using 5 μg of GST. *C*, densitometric analysis of ZO-1 bands from three different experiments described in *panel B*. In each experiment, ZO-1 band density for GST-cOcl-C$_{WT}$ incubated without ATP was designated to 100, and corresponding bands in other groups were normalized as a percent of that number. Values are the mean $\pm$ S.E. (*n* = 3). *Asterisks* indicate the values that are significantly (*p* < 0.05) different from corresponding value for −ATP group.

(Fig. 9*B*). ZO-1 distribution in hydrogen peroxide-treated cell monolayers paralleled the distribution of GFP.

Tyr-398- and Tyr-402-phosphorylated Occludin Results in Loss of Interaction with ZO-1 in MDCK Cell Monolayers—To confirm the H$_2$O$_2$-induced phosphorylation of occludin in the cell, we evaluated H$_2$O$_2$-induced Tyr-phosphorylation of GFP-hOcl$_{WT}$, GFP-hOcl$_{Y398A/Y402A}$, and GFP-hOcl$_{Y398D/Y402D}$ in MDCK cell monolayers. Immunoprecipitation of GFP followed by immunoblot analysis in H$_2$O$_2$-treated cells

expressing GFP-hOcl$_{WT}$ indicated that occludin was phosphorylated on Tyr residues (Fig. 9*C*). However, GFP-hOcl$_{Y398A/Y402A}$ and GFP-hOcl$_{Y398D/Y402D}$ were not Tyr-phosphorylated in H$_2$O$_2$-treated cells.

Coimmunoprecipitation studies (Fig. 9*D*) indicated that ZO-1 coimmunoprecipitated with GFP-Ocl$_{WT}$ and GFP-hOcl$_{Y398A/Y402A}$, whereas ZO-1 failed to co-immunoprecipitate with GFP-hOcl$_{Y398D/Y402D}$, indicating that phosphorylation of Tyr-398 and Tyr-402 results in loss of interaction with ZO-1 in MDCK cells.

DISCUSSION

A significant body of evidence suggests that Tyr phosphorylation of TJ proteins may play an important role in the regulation of epithelial TJs. Occludin is highly phosphorylated on Ser and Thr residues in the intact epithelium, and Tyr phosphorylation is undetectable (38). Previous studies, however, demonstrated that occludin undergoes Tyr phosphorylation during the disruption of TJs by hydrogen peroxide (11, 39). Furthermore, a recent *in vitro* study demonstrated that Tyr phosphorylation of the C-terminal region of occludin reduces its ability to interact with ZO-1, a TJ plaque protein (25). In the present study we identified the Tyr phosphorylation sites in the C-terminal region of occludin and demonstrated their role in regulation of ZO-1 binding.

The Tyr phosphorylation sites in the C-terminal region of chicken occludin were determined by mass spectrometric analysis of phospho-occludin. Mass analysis of phosphopeptide extracts from tryptic digests detected the presence of one phosphopeptide corresponding to the predicted peptide fragment of chicken occludin (amino acids 371–393) with phospho-Tyr residues. There are two Tyr residues within this sequence (Tyr-379 and 383), which were found to be phosphorylated as the mass of this peptide was 160 daltons greater than the predicted mass value. Another phosphopeptide detected by MALDI showed a molecular mass of 2915.7, which is 156 daltons greater than the predicted mass of the monophosphate peptide fragment. LC/MS/MS analysis determined that this peptide corresponds to the sequence 370–
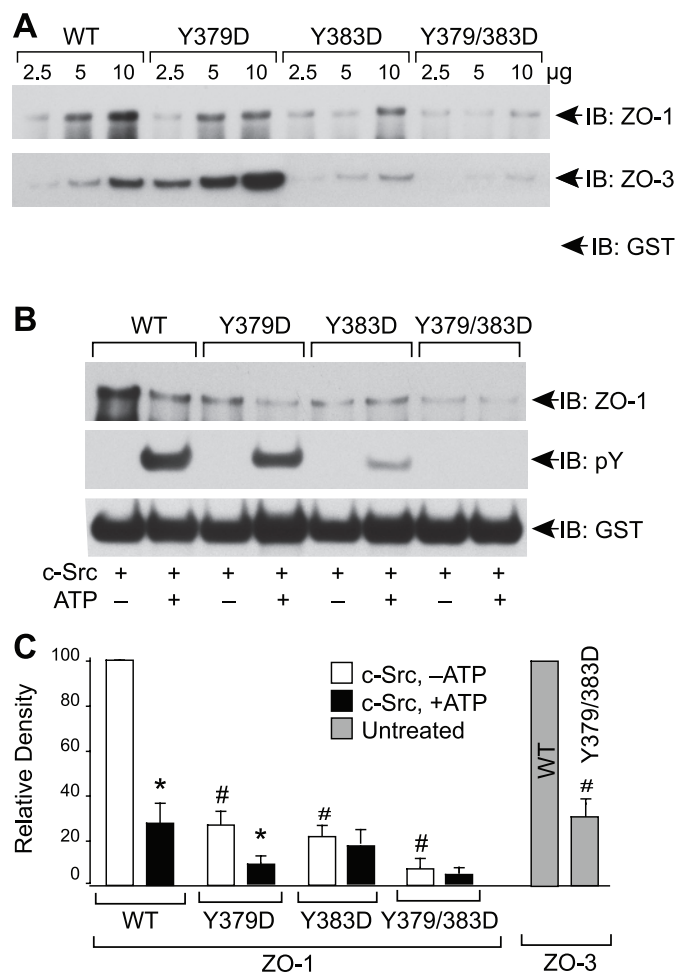
FIGURE 5. Y379D and Y383D in chicken occludin attenuates its binding to ZO-1. *A*, GST-cOcl-C$_{WT}$, GST-cOcl-C$_{Y379D}$, GST-cOcl-C$_{Y383D}$, and GST-cOcl-C$_{Y379/383D}$ were analyzed for ZO-1 binding by GST pulldown assay. GST pulldown assays were immunoblotted (*IB*) for ZO-1 and GST. *B*, GST-cOcl-C, GST-cOcl-C$_{Y379D}$, GST-cOcl-C$_{Y383D}$, and GST-cOcl-C$_{Y379/383D}$ were incubated with c-Src in the absence or presence of ATP. Ten μg each of phosphorylated and non-phosphorylated occludins were analyzed for ZO-1 binding by GST pulldown assay. GST pulldown assays were immunoblotted for ZO-1, p-Tyr, and GST. *C*, densitometric analysis of ZO-1 bands from three different experiments described as in *panel B* and selected ZO-3 bands in *panel A*. In each experiment, ZO-1 (or ZO-3) band density for GST-cOcl-C incubated without ATP was designated to 100, and corresponding bands in other groups were normalized as a percent of that number. Values are the mean ± S.E. (*n* = 3). *Asterisks* indicate the values that are significantly (*p* < 0.05) different from corresponding value for −ATP group, and the symbols # indicate the values that are significantly different (<0.05) from corresponding value for WT group.

FIGURE 6. Mutation of Tyr-398 and Tyr-402 in human occludin attenuates its phosphorylation and altered regulation of ZO-1 binding. *A*, GST-hOcl-C$_{WT}$, GST-hOcl-C$_{Y398F/Y402F}$, and GST-hOcl-C$_{Y398D/Y402D}$ were incubated with c-Src in the absence or presence of ATP. Five μg of phosphorylated or non-phosphorylated occludin was analyzed for ZO-1 binding by GST pulldown assay. GST pulldown assays were immunoblotted (*IB*) for ZO-1, p-Tyr, and GST. *B*, five μg of phosphorylated or non-phosphorylated GST-hOcl-C and GST-hOcl-C$_{Y398A/Y402A}$ were incubated with c-Src in the absence or presence of ATP and analyzed for ZO-1 binding by GST pulldown assay. GST pulldown assays were immunoblotted for ZO-1, p-Tyr, and GST. *C*, densitometric analysis of ZO-1 bands from three different experiments described in *panel B*. In each experiment, ZO-1 band density for GST-cOcl-C incubated without ATP was designated to 100, and corresponding bands in other groups were normalized as a percent of that number. Values are the mean ± S.E. (*n* = 3). The *asterisk* indicates the value that is significantly (*p* < 0.05) different from corresponding value for -ATP group. # indicates the values that are significantly (*p* < 0.05) different from value for non-phosphorylated wild type occludin.

393 of chicken occludin with an extra Arg (Arg-370) at the N terminus compared with the predicted 371–393 fragment. This is possibly caused by a misdigestion by trypsin due to the presence of sequential Arg residues in this region of the occludin sequence. LC/MS/MS analysis also detected two types of 2915.2-dalton peptides; one in which Tyr-379 was phosphorylated and another in which Tyr-383 was phosphorylated. Therefore, the sequences of all three phosphopeptides identified in the study demonstrate that Tyr-379 and Tyr-383 are the phosphorylation sites in chicken occludin; Tyr-398 and Tyr-402 are the corresponding tyrosines in human occludin. These two tyrosines are located in a highly conserved sequence of occludin HYETDYTT. BLAST analysis of this sequence demonstrated
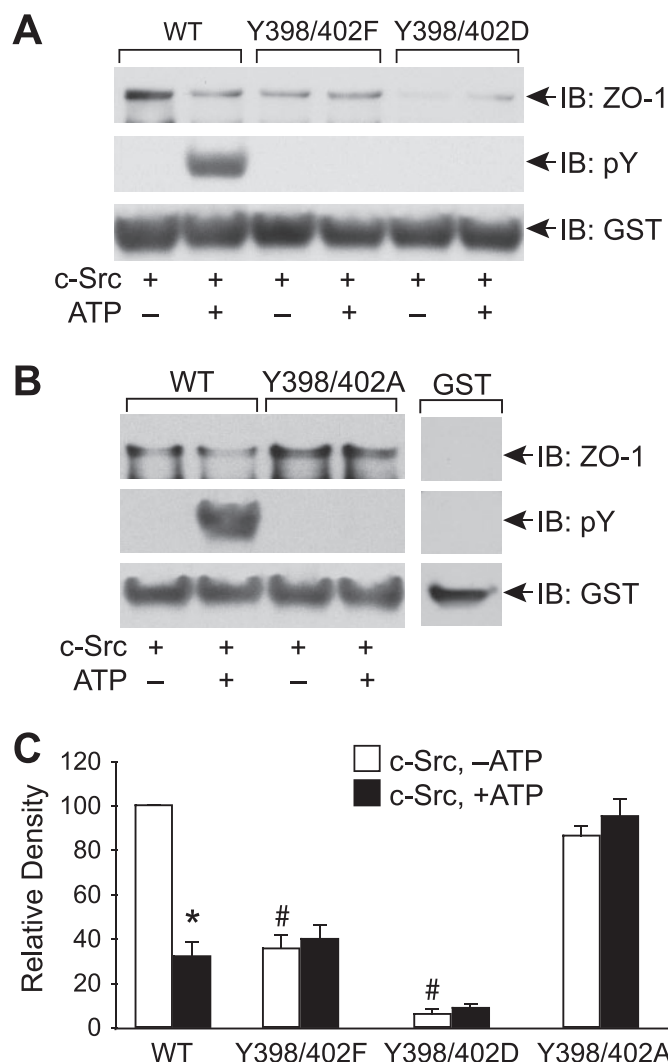
that this is a unique motif that is not present in other proteins, including claudins.

Deletion of HYETDYTT (378–385) from chicken occludin abrogated c-Src-induced Tyr-phosphorylation of the occludin C-terminal region, confirming the mass spectrometric data that Tyr-379 and Tyr-383 are the phosphorylation sites in chicken occludin. Point mutation of Tyr-379 or Tyr-383 to phenylalanine resulted in a partial decrease in c-Src-induced Tyr-phosphorylation. Decrease in Tyr phosphorylation was greater in Y383F mutants compared with that in Y379F mutants, sug-
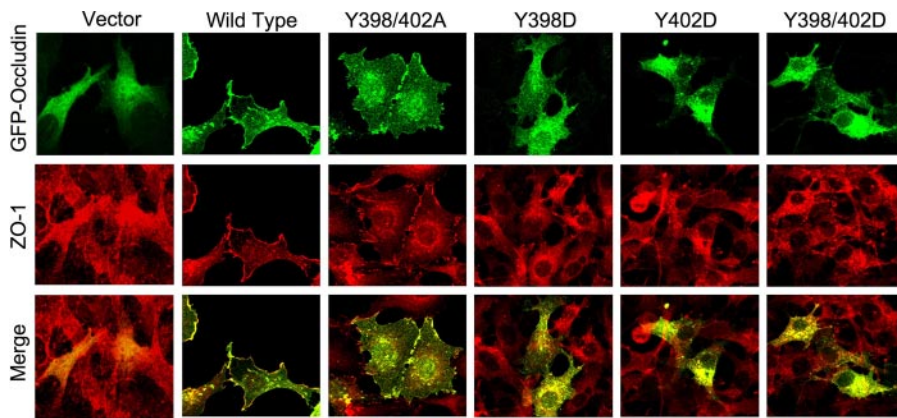
FIGURE 7. **Y398D and Y402D mutations in human occludin prevents its localization at the plasma membrane and cell-cell contact sites in Rat-1 cells.** GFP-hOcl$_{WT}$, GFP-cOcl$_{Y398A/Y402A}$, GFP-cOcl$_{Y398D}$, GFP-cOcl$_{Y402D}$, GFP-cOcl$_{Y398D/Y402D}$, and pEGFP empty vector were expressed in Rat-1 cells. Subcellular localization was examined by immunofluorescence confocal microscopy by double labeling for GFP and ZO-1.
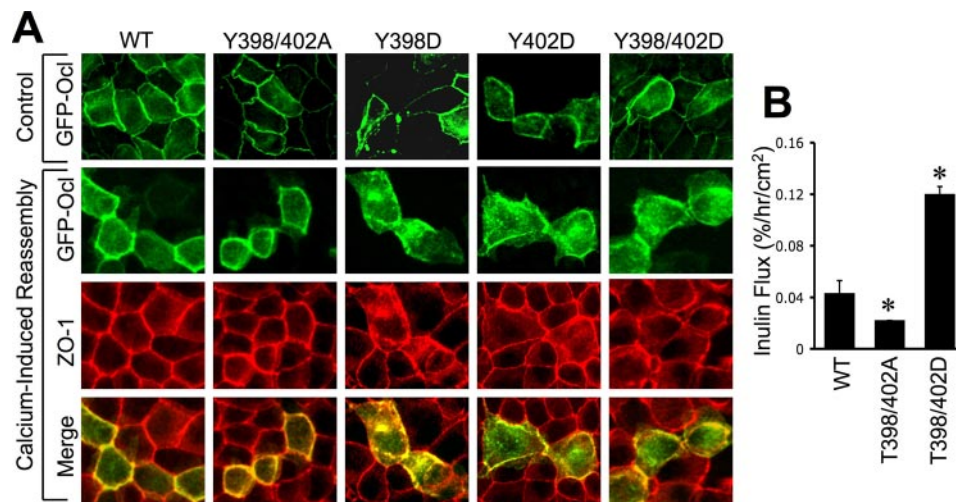

FIGURE 8. **Y398D and Y402D mutations in human occludin prevents its assembly at the intercellular junctions in MDCK cells.** *A*, 360q-length human occludin, GFP-hOcl$_{WT}$, GFP-hOcl$_{Y398A/Y402A}$, GFP-cOcl$_{Y398D/}$GFP-cOcl$_{Y402D}$, and GFP-hOcl$_{Y398D/Y402D}$ were expressed in MDCK cells. Subcellular localization was examined 1 h after calcium replacement by immunofluorescence confocal microscopy by double labeling for GFP and ZO-1. *B*, inulin permeability was measured in cell monolayers expressing GFP-hOcl$_{WT}$, GFP-hOcl$_{Y398A/Y402A}$, and GFP-hOcl$_{Y398D/Y402D}$. Values are the mean $\pm$ S.E. ($n = 4$). *Asterisks* indicate the values that are significantly ($p < 0.05$) different from corresponding value for GFP-hOcl$_{WT}$.

gesting that Tyr-383 is a preferred phosphorylation site. Double mutation of Tyr-379 and Tyr-383 abolished c-Src-induced Tyr phosphorylation. Similarly, mutation of Tyr-398 and Tyr-402 in the C-terminal region of human occludin also abrogated the c-Src-induced Tyr phosphorylation. Previous studies showed that c-Src plays an important role in hydrogen peroxide-induced disruption of TJs and barrier dysfunction in Caco-2 cell monolayers (11). Expression of inactive c-Src significantly reduced hydrogen peroxide-induced Tyr-phosphorylation of occludin and TJ disruption, suggesting that c-Src-induced Tyr-phosphorylation may be involved in this process. The present study suggests that hydrogen peroxide may induce phosphorylation of Tyr-379 and Tyr-383 in Caco-2 cells. A previous study demonstrated that Tyr phosphorylation of the C-terminal region of occludin results in the loss of its interaction with ZO-1 (25). ZO-1, a major adaptor protein of TJs, interacts with C-terminal region of occludin on one hand and with actin cytoskeleton on the other (12, 14).

The interaction between the C-terminal region of occludin and ZO-1 is crucial for the assembly and the maintenance of occludin at the TJs (14). Truncation of the C-terminal region of occludin resulted in a loss of its interaction with ZO-1 and prevented its assembly into TJs. In the present study we determined the role of phosphorylation of specific Tyr residues in the C-terminal region of occludin in the regulation of its interaction with ZO-1. GST pulldown assays demonstrated that C-terminal regions of both chicken and human occludin bind to ZO-1. Deletion of the sequence HYET-DYTT in chicken occludin resulted in a significant reduction in binding to ZO-1 at higher concentrations of occludin; however, at low concentrations the deletion mutant bound to ZO-1 at a similar level to that of the wild type occludin. When wild type occludin C-terminal domain was incubated with c-Src and ATP, there was a significant reduction in ZO-1 binding; however, this was not observed with the deletion mutant, indicating that the phosphorylation of Tyr-379 and Tyr-383 is important in the regulation of interaction between occludin and ZO-1. This was confirmed by point mutations of Tyr-379 and -383. Y379F mutation partially reduced c-Src-induced regulation of ZO-1 binding, whereas Y383F or Y379F/Y383F mutation completely attenuated c-Src-induced regula-

tion of ZO-1 binding. Similarly, Y398F/Y402F mutation in human occludin attenuated c-Src-induced regulation of ZO-1 binding. However, Y398F/Y402F mutation by itself resulted in significant reduction in ZO-1 binding. On the other hand, Y398A/Y402A mutation did not affect ZO-1 binding in the absence or presence of c-Src. Therefore, the results of this study demonstrate that Tyr-398 and Tyr-402 are important in regulation of ZO-1 binding by human occludin.

The crystal structure of the occludin C-terminal region (383–522) has been determined recently (15). This coiled-coil region C-terminal to the Tyr phosphorylation sites does bind to ZO-1 quite well. This indicates that the main function of the phosphorylation is not ZO-1 binding; rather, it plays a role in the regulation of ZO-1 binding. Similar to ZO-1 binding, ZO-3 binding to GST-hOcl-C was also altered by mutation of Tyr-398 and -402. Interestingly, ZO-3 binding to Y398F mutant was greater than its binding to GST-hOcl-C$_{WT}$. However, at present, the reason for this enhanced binding is not clear and needs further studies.
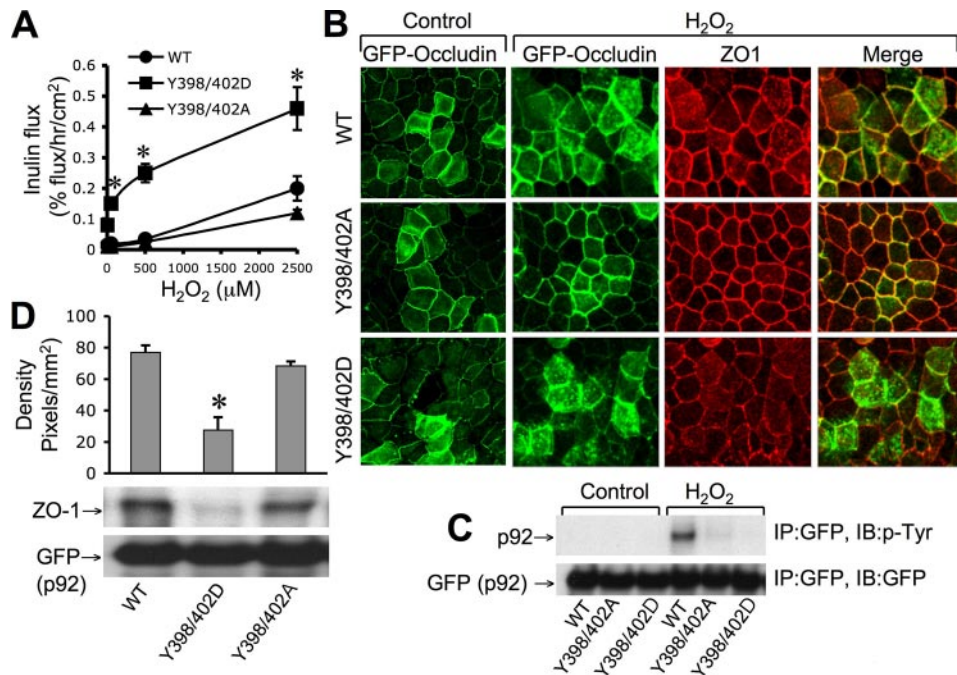
FIGURE 9. **Y398D/Y402D mutation of occludin sensitizes MDCK cell monolayers for hydrogen peroxide-induced disruption of TJs.** *A* and *B*, MDCK cell monolayers that express GFP-hOcl$_{WT}$, GFP-hOcl$_{Y398A/Y402A}$, or GFP-hOcl$_{Y398D/Y402D}$ were exposed to varying concentrations of hydrogen peroxide. Inulin permeability was measured 1 h after hydrogen peroxide (*A*), and fixed cell monolayers were double-stained for GFP and ZO-1 by the immunofluorescence method (*B*). *C*, MDCK cell monolayers that express GFP-hOcl$_{WT}$, GFP-hOcl$_{Y398A/Y402A}$, or GFP-hOcl$_{Y398D/Y402D}$ were incubated with or without (control) hydrogen peroxide for 1 h. Anti-GFP immunocomplexes prepared under denatured conditions were immunoblotted (*IB*) for p-Tyr and GFP. The *arrow* with p92 label corresponds to GFP-occludin. *IP*, immunoprecipitates. *D*, anti-GFP immunocomplexes prepared under non-denaturing conditions from MDCK cells expressing wild type or mutant occludins were immunoblotted for ZO-1 and GFP. Density of ZO-1 bands from three different experiments was measured. The *arrow* with *p92* label corresponds to GFP-occludin.

To determine the effect of Tyr-398 or Tyr-402 phosphorylation on the assembly of occludin into intercellular junctions, we induced point mutations to GFP-tagged full-length human occludin. The GFP-hOcl$_{WT}$ and its mutants, GFP-hOcl$_{Y398/Y402A}$, GFP-hOcl$_{Y398/Y402D}$, and the corresponding single mutants were transfected into Rat-1 fibroblasts or MDCK cells. Confocal immunofluorescence microscopy demonstrated that the GFP-hOcl$_{WT}$ and its Y398/Y402A mutant were localized at the plasma membrane of Rat-1 cells, forming intercellular contact sites. Rat-1 cells express high levels of ZO-1, but it is predominantly localized in the intracellular compartment. However, transfection of GFP-hOcl$_{WT}$ or GFP-hOcl$_{Y398/Y402A}$ induced a recruitment of ZO-1 at the plasma membrane and the intercellular contact sites. Y398A/Y402A mutation did not alter the distribution of occludin at the plasma membranes. However, Y398D, Y402D, and Y398/Y402D mutants of occludin failed to localize at the plasma membrane or cell-cell contact sites; rather, they were distributed in the intracellular compartment. This indicates that mimicking the phosphorylation of Tyr-398 and Tyr-402 by mutation to aspartic acid results in the loss of its ability to assemble at the plasma membranes and cell-cell contact sites. This may be due to the loss of its ability to bind to ZO-1.

A significant portion of GFP-occludin in vesicular structure did appear near the plasma membrane, suggesting that the mutation did not result in a defect in its ability to integrate into the plasma membrane; rather, these occludin mutants are internalized into the cells due to the lack of their interaction

with ZO-1 and inability to integrate into TJ structure. Both single mutants, Y398D and Y402D, similarly failed to localize at the intercellular junctions, indicating that phosphorylation of either Tyr residues is enough to alter its ability to bind ZO-1 and integrate into TJs. *In vitro* phosphorylation and ZO-1 binding studies indicated that Tyr-383 is more important than Tyr-379 in chicken occludin. However, this is in contrast to cell data, which shows that both Tyr-398 and Tyr-402 in human occludin are important for its localization at the cell-cell contact sites. This may be explained by the lower preference of c-Src for Tyr-379 compared with Tyr-383. In the cell, Tyr-379 may be phosphorylated by some other tyrosine kinase.

In MDCK cells, wild type and Y398A/Y402A mutant occludin were localized at the intercellular junctions. However, during the early stages of TJ assembly by calcium replacement, we saw a delay in the organization of GFP-hOcl$_{Y398D/Y402D}$ at the intercellular junctions. One hour after calcium replacement, Y398D/Y402D mutant occludin was distributed predominantly in the intracellular compartment, whereas WT and Y398A/Y402A mutant occludin were organized at the intercellular junctions. This confirmed that phosphorylation of Tyr-398 and Tyr-402 of occludin does prevent its ability to integrate into the TJs. The organization of Y398D/Y402D mutant at the intercellular junctions may be mediated by dimerization of mutant with the endogenous occludin. Expression of Y398D/Y402D mutant of occludin did disrupt the junctional distribution of ZO-1. This dominant negative effect is evident only at higher levels of mutant expression. The expression of mutant in relation to endogenous occludin is difficult to assess. However, ZO-1 redistribution was seen only in cells with higher level of mutant expression. Therefore, it is not clear whether such an effect can be seen at endogenous levels of phospho-occludin.

Furthermore, MDCK cell monolayers that express Y398D/Y402D mutant of occludin were dramatically more sensitive to hydrogen peroxide-induced disruption of barrier function, whereas cell monolayers expressing Y398A/Y402A mutant occludin showed significant resistance to hydrogen peroxide compared with cell monolayers expressing wild type occludin. The present study also shows that hydrogen peroxide failed to induce Tyr phosphorylation in MDCK cell monolayers, demonstrating that Tyr-398 and Tyr-402 are the phosphorylation sites in hydrogen peroxide-treated cells. The loss of co-immunoprecipitation of ZO-1 with GFP-hOcl$_{Y398D/Y402D}$ in MDCK cells confirms our observation made in *in vitro* studies that

phosphorylation of Tyr-398 and Tyr-402 does prevent its interaction with ZO-1.

As shown in Fig. 9, the GFP-hOcl$_{Y398D/Y402D}$ eventually tends to organize at the intercellular junctions, although not as discretely as GFP-hOcl$_{WT}$ or GFP-hOcl$_{Y398A/Y402A}$. This is possibly due to oligomerization of GFP-hOcl$_{Y398D/Y402D}$ with the endogenous occludin. The inulin flux in hydrogen peroxide-treated cell monolayers that express GFP-hOcl$_{Y398D/Y402D}$ is significantly higher than that in cells that express GFP-hOcl$_{WT}$ or GFP-hOcl$_{Y398A/Y402A}$. The mechanism for greater sensitivity to hydrogen peroxide or delayed assembly is not clear at this point. However, we speculate that mixed oligomerization of GFP-Ocl$_{Y398D/Y402D}$ and endogenous occludin facilitates the dissociation of ZO-1 by hydrogen peroxide due to weak interaction between GFP-Ocl$_{Y398D/Y402D}$ with ZO-1; this may work synergistically with the hydrogen peroxide-induced Tyr phosphorylation of endogenous occludin and loss of its interaction with ZO-1. In summary, this study identifies Tyr-398 and Tyr-402 as the phosphorylation sites in human occludin and demonstrates that phosphorylation of these Tyr residues results in the loss of interaction between occludin and ZO-1 and attenuation of its integration into the epithelial TJs.

REFERENCES

1. Gonzalez-Mariscal, L., Betanzos, A., Nava, P., and Jaramillo, B. E. (2003) *Prog. Biophys. Mol. Biol.* **81,** 1–44
2. Gonzalez-Mariscal, L., Lechuga, S., and Garay, E. (2007) *Prog. Histochem. Cytochem.* **42,** 1–57
3. Berkes, J., Viswanathan, V. K., Savkovic, S. D., and Hecht, G. (2003) *Gut* **52,** 439–451
4. Laukoetter, M. G., Bruewer, M., and Nusrat, A. (2006) *Curr. Opin. Gastroenterol.* **22,** 85–89
5. Coyne, C. B., Vanhook, M. K., Gambling, T. M., Carson, J. L., Boucher, R. C., and Johnson, L. G. (2002) *Mol. Biol. Cell* **13,** 3218–3234
6. Balkovetz, D. F. (2006) *Am. J. Physiol.* **290,** F572–F579
7. Ma, T. Y., Iwamoto, G. K., Hoa, N. T., Akotia, V., Pedram, A., Boivin, M. A., and Said, H. M. (2004) *Am. J. Physiol.* **286,** G367–G376
8. Stevens, C., Walz, G., Singaram, C., Lipman, M. L., Zanker, B., Muggia, A., Antonioli, D., Peppercorn, M. A., and Strom, T. B. (1992) *Dig. Dis. Sci.* **37,** 818–826
9. Wang, F., Schwarz, B. T., Graham, W. V., Wang, Y., Su, L., Clayburgh, D. R., Abraham, C., and Turner, J. R. (2006) *Gastroenterology* **131,** 1153–1163
10. Rao, R. K., Baker, R. D., and Baker, S. S. (1999) *Biochem. Pharmacol.* **57,** 685–695
11. Basuroy, S., Sheth, P., Kuppuswamy, D., Balasubramanian, S., Ray, R. M., and Rao, R. K. (2003) *J. Biol. Chem.* **278,** 11916–11924
12. Rao, R. K. (2008) *Front. Biosci.* **13,** 7210–7226
13. Schneeberger, E. E., and Lynch, R. D. (2004) *Am. J. Physiol.* **286,** C1213–C1228
14. Furuse, M., Itoh, M., Hirase, T., Nagafuchi, A., Yonemura, S., Tsukita, S., and Tsukita, S. (1994) *J. Cell Biol.* **127,** 1617–1626
15. Li, Y., Fanning, A. S., Anderson, J. M., and Lavie, A. (2005) *J. Mol. Biol.* **352,** 151–164
16. Itoh, M., Morita, K., and Tsukita, S. (1999) *J. Biol. Chem.* **274,** 5981–5986
17. Wittchen, E. S., Haskins, J., and Stevenson, B. R. (1999) *J. Biol. Chem.* **274,** 35179–35185
18. Haskins, J., Gu, L., Wittchen, E. S., Hibbard, J., and Stevenson, B. R. (1998) *J. Cell Biol.* **141,** 199–208
19. Itoh, M., Furuse, M., Morita, K., Kubota, K., Saitou, M., and Tsukita, S. (1999) *J. Cell Biol.* **147,** 1351–1363
20. Zhong, Y., Saitoh, T., Minase, T., Sawada, N., Enomoto, K., and Mori, M. (1993) *J. Cell Biol.* **120,** 477–483
21. Citi, S., Sabanay, H., Jakes, R., Geiger, B., and Kendrick-Jones, J. (1998) *Nature* **333,** 272–275
22. Keon, B. H., Schafer, S., Kuhn, C., Grund, C., and Franke, W. W. (1996) *J. Cell Biol.* **134,** 1003–1018
23. Miyoshi, J., and Takai, Y. (2005) *Adv. Drug Delivery Rev.* **57,** 815–855
24. Andreeva, A. Y., Krause, E., Muller, E. C., Blasig, I. E., and Utepbergenov, D. I. (2001) *J. Biol. Chem.* **276,** 38480–38486
25. Kale, G., Naren, A. P., Sheth, P., and Rao, R. K. (2003) *Biochem. Biophys. Res. Commun.* **302,** 324–329
26. Nusrat, A., Chen, J. A., Foley, C. S., Liang, T. W., Tom, J., Cromwell, M., Cliff, Q., and Randall, J. M. (2000) *J. Biol. Chem.* **275,** 29816–29822
27. Chen, Y. H., Lu, Q., Goodenough, D. A., and Jeansonne, B. (2002) *Mol. Biol. Cell* **13,** 1227–1237
28. Basuroy, S., Seth, A., Elias, B., Naren, A. P., and Rao, R. (2006) *Biochem. J.* **393,** 69–77
29. Seth, A., Sheth, P., Elias, B. C., and Rao, R. K. (2007) *J. Biol. Chem.* **282,** 11487–11498
30. Stuart, R. O., Sun, A., Panichas, M., Hebert, S. C., Brenner, B. M., and Nigam, S. K. (1994) *J. Cell. Physiol.* **159,** 423–433
31. Sheth, P., Basuroy, S., Li, C., Naren, A. P., and Rao, R. K. (2003) *J. Biol. Chem.* **278,** 49239–49245
32. Nusrat, A., Giry, M., Turner, J. R., Colgan, S. P., Parkos, C. A., Carnes, D., Lemichez, E., Boquet, P., and Madara, J. L. (1995) *Proc. Natl. Acad. Sci. U. S. A.* **92,** 10629–10633
33. Takaishi, K., Sasaki, T., Hirokazu, K., Nishioka, H., and Takai, Y. (1997) *J. Cell Biol.* **139,** 1047–1059
34. Saitou, M., Furuse, M., Sasaki, H., Schulzke, J. D., Fromm, M., Takano, H., Noda, T., and Tsukita S. (2000) *Mol. Biol. Cell* **11,** 4131–4142
35. Fujimoto, K. (1995) *J. Cell Sci.* **108,** 3443–3449
36. Furuse, M., Hirase, T., Itoh, M., Nagafuchi, A., Yonemura, S., Tsukita, Sa., and Tsukita, Sh. (1993) *J. Cell Sci.* **123,** 1777–1788
37. Ando-Akatsuka, Y., Saitou, M., Hirase, T., Kishi, M., Sakakibara, A., Itoh, M., Yonemura, S., Furuse, M., and Tsukita, S. (1996) *J. Cell Biol.* **133,** 43–47
38. Sakakibara, A., Furuse, M., Saitou, M., Ando-Akatsuka, Y., and Tsukita, S. (1997) *J. Cell Biol.* **137,** 1393–1401
39. Rao, R. K., Basuroy, S., Rao, V. U., Karnaky, K. J., and Gupta, A. (2002) *Biochem. J.* **368,** 471–481
40. Atkinson, K. J., and Rao, R. K. (2001) *Am. J. Physiol.* **280,** G1280–G1288